MILLIMETER-WAVE PROPAGATION IN THE MESOSPHERE

George A. Hufford and Hans J. Liebe*

At heights between 30 and 100 km above Earth, the oxygen absorption lines near 60 GHz together with the geomagnetic field cause the atmosphere to become an anisotropic medium. This report discusses why this is so and how to compute the consequent effects. It describes the computer program ZEEMAN, which allows the user to display in either graphical or tabular form many aspects of how radio waves propagate through this medium.

Key words: anisotropic media; mesosphere; millimeter waves; oxygen absorption lines; polarization; radio propagation; Zeeman effect

1. INTRODUCTION

The mesosphere is that portion of Earth's atmosphere that lies between the stratosphere and the thermosphere from somewhat above 30 km in altitude to less than 100 km. The air is tenuous, and pressures vary from 1 to 10^{-4} kPa. Nevertheless, the oxygen absorption lines near 60 GHz are still strong enough to affect radio propagation.

Because the pressure is low, the lines are very sharp and a new phenomenon appears. This is the Zeeman effect induced by the geomagnetic field. Each line splits into a number of sublines; and how these sublines react to an electromagnetic field depends on the polarization of that field. There is, therefore, a small portion of the spectrum where the medium is anisotropic so that radio waves propagating through it are subject to such consequences as polarization discrimination and Faraday rotation. The physical reasons for this behavior are discussed in Townes and Schawlow (1955, especially Chapter 11). Engineering characterizations are given in Gautier (1967), Lenoir (1968), Liebe (1981, 1983), Hartman and Künzi (1983), and Rosenkranz and Staelin (1988). This report will summarize these results and show how they may be used to describe radio wave propagation in this medium. The final sections describe a computer program ZEEMAN, which allows a user to choose a scenario involving radio propagation at a point above Earth and to compute properties of the resultant propagation effects.

---

*The authors are with the Institute for Telecommunication Sciences, National Telecommunications and Information Administration, U.S. Department of Commerce, Boulder, CO 80303.

2. THE OXYGEN ABSORPTION LINES NEAR 60 GHz

In this section, we define a model describing the electromagnetic properties of the mesospheric atmosphere. We begin with the case when there is no geomagnetic field, and we shall describe the nearly 40 oxygen obsorption lines that lie near 60 GHz. Later, we shall consider the effect of a static magnetic field on a single one of these lines.

2.1 Line Properties in the Absence of a Magnetic Field

Gaseous molecules tumble about in space and vibrate internally, and the motion requires energy that is confined to a set of discrete quantum levels. A transition between two of these levels is accompanied by the absorption or emission of electromagnetic energy at a precise frequency, thus marking out a spectral line.

Most molecules that have absorption lines at radio frequencies interact with the electromagnetic field because they have an electric dipole moment. The O_2 molecule, however, is quite symmetrical with its 16 electrons evenly distributed. It has no electric dipole moment and therefore cannot interact with the electric field. On the other hand, the molecule in its normal state does have one rather subtle asymmetry--nine of its electrons spin in one direction while seven spin in the other. The resultant total spin provides a *magnetic* dipole moment. The oxygen molecule is paramagnetic and interacts with the magnetic component of the electromagnetic field.

Rotational energy levels of a linear gaseous molecule (having one principle moment of inertia) arise from the angular momentum associated with its tumbling action. Approximate values are given by the formula $BK(K+1)$, where B is related to the moment of inertia of the molecule and the "quantum number" K may be any nonnegative integer. In particular, this is true of the O_2 molecule except that symmetry again intervenes, and because of the Pauli exclusion principle, it turns out that only odd K are allowed. This produces the "orbital angular momentum" levels.

The 60-GHz lines do not come directly from those levels but from their "fine structure." The electron spin again enters the picture and now becomes an additional independent component of the angular momentum. Since electrons have spin 1/2, the total electron spin of the normal oxygen molecule is 1, and this adds vectorially into the resultant angular momentum. It follows that

for each K, the "total angular momentum" takes on values J=K-1, K, and K+1, so that each energy level has split into three.

When these three fine structure levels interact with an electromagnetic field, there are "selection rules" which in this case say that transitions can take place only between adjacent quantum numbers. Thus there can be transitions between the K and K+1 levels and between the K and K-1 levels. These produce what are called the K^+ and K^- absorption lines, respectively.

To the engineer, these absorption lines show themselves as resonances in the complex refractivity of the atmosphere. Following Liebe (1983), we write

$$N = N_s + N'(f) + iN''(f) \tag{1}$$

where N_s is a frequency-independent refractivity, N' is a refractive dispersion, and N'' is the absorption term. These are all small numbers and normally they are measured in parts per million (sometimes called N-units). Free propagation of a plane wave in the z-direction is then given by

$$E(z) = \exp[ikz(1 + N)]\, E_o \tag{2}$$

where $E(z)$ is the electric field at z, E_o is the initial electric field at $z = 0$, and $k = 2\pi f/c$ is the free space wave number. In more practical terminology, we have the specific attenuation α, the excess phase lag β, and the specific delay time τ given by

$$\begin{aligned} \alpha &= 0.1820\ f\ N''(f) && \text{dB/km}, \\ \beta &= 1.2008\ f\ [N_s + N'(f)] && \text{deg/km}, \\ \tau &= 3.3356\ [N_s + N'(f)] && \text{ps/km}, \end{aligned} \tag{3}$$

where f is to be measured in gigahertz and the refractivities in parts per million.

In this report, we shall restrict ourselves to frequencies near 60 GHz and to conditions that resemble the atmosphere above 30 km altitude where the air is dry and the environmental parameters of concern are pressure P and temperature T. We suppose P is measured in kilopascal, and define a "relative inverse temperature," $\theta = 300/T$, where T is the absolute temperature in kelvin. Then our model for the refractivity sets

$$N_s = 2.5892\ P\theta \qquad \text{ppm} \tag{4}$$

and

$$N' + iN'' = \sum_n (SF)_n \qquad \text{ppm}\ , \tag{5}$$

where S is a line strength and F a Lorentzian line shape function

$$F(f) = 1/(\nu_o - f - i\gamma) \tag{6}$$

with the line center frequency ν_o and the line width γ. One measures S in kilohertz and the frequencies in the denominator of F in gighertz, thus building in a factor of 10^6 to produce the refractivity units.

The center frequencies have fixed values but the strengths and widths are to be calculated from

$$S = a_1 P\theta^3 \exp[a_2(1 - \theta)] \qquad \text{kHz} \tag{7}$$

and

$$\gamma = a_3 P\theta^{0.8} \qquad \text{GHz} \tag{8}$$

The line center frequencies ν_o (Endo and Mizushima, 1982) and the spectroscopic coefficients a_1, a_2 (Liebe, 1983), and a_3 (Liebe et al., 1977) are listed in Table 1 for some 40 of these absorption lines.

Table 2 gives representative values of temperature and pressure at the high altitudes of interest here. They are taken from the U.S. Standard Atmosphere 76 (COESA, 1976) and are the values we shall assume throughout.

We note from Table 1 that most of the center frequencies are between 50 and 70 GHz. One exception is the 1^- line. It lies near 119 GHz, but we still include it as one of the lines of our study.

Also from Table 1 we note that the lines are generally separated by about 500 MHz. Since line widths above 30 km are 20 MHz or less, each line will be well isolated. Occassionally, however, the K^+ and K^- lines happen to fall especially close, forming what are called "doublets." These doublets should probably be treated together. There are four of them and they are flagged in Table 1.

From (6) we observe that the imaginary part of SF(f) reaches its maximum of S/γ at the center frequency. And from (7) and (8) we see that this ratio is independent of pressure. In addition, its dependence on temperature is not

Table 1. Line Frequencies and Coefficients for Microwave Transitions of O_2 in Air

K±	ν_o	a_1	a_2	a_3
	GHz	kHz/kPa $\times 10^{-6}$		GHz/kPa $\times 10^{-3}$
39-	49.962257	0.34	10.724	8.50
37-	50.474238	0.94	9.694	8.60
35-	50.987749	2.46	8.694	8.70
33-	51.503350	6.08	7.744	8.90
31-	52.021410	14.14	6.844	9.20
29-	52.542394	31.02	6.004	9.40
27-	53.066907	64.10	5.224	9.70
25-	53.595749	124.70	4.484	10.00
23-	54.130000	228.00	3.814	10.20
21-	54.671159	391.80	3.194	10.50
19-	55.221367	631.60	2.624	10.79
17-	55.783802	953.50	2.119	11.10
1+ |	56.264775	548.90	0.015	16.46
15- |	56.363389	1344.00	1.660	11.44
13-	56.968206	1763.00	1.260	11.81
11-	57.612484	2141.00	0.915	12.21
9- |	58.323877	2386.00	0.626	12.66
3+ |	58.446590	1457.00	0.084	14.49
7-	59.164207	2404.00	0.391	13.19
5+	59.590983	2112.00	0.212	13.60
5- |	60.306061	2124.00	0.212	13.82
7+ |	60.434776	2461.00	0.391	12.97
9+	61.150560	2504.00	0.626	12.48
11+	61.800154	2298.00	0.915	12.07
13+ |	62.411215	1933.00	1.260	11.71
3- |	62.486260	1517.00	0.083	14.68
15+	62.997977	1503.00	1.665	11.39
17+	63.568518	1087.00	2.115	11.08
19+	64.127767	733.50	2.620	10.78
21+	64.678903	463.50	3.195	10.50
23+	65.224071	274.80	3.815	10.20
25+	65.764772	153.00	4.485	10.00
27+	66.302091	80.09	5.225	9.70
29+	66.836830	39.46	6.005	9.40
31+	67.369598	18.32	6.845	9.20
33+	67.900867	8.01	7.745	8.90
35+	68.431005	3.30	8.695	8.70
37+	68.960311	1.28	9.695	8.60
39+	69.489021	0.47	10.720	8.50
1-	118.750343	945.00	0.009	16.30

Table 2. Temperature and Pressure in the Mesosphere
(U.S. Standard Atmosphere, 1976)

Altitude	Atmosphere	Temperature	Pressure	Line Shape
km		°C	Pa	
30	Stratosphere	-46.64	1197	Lorentz
35		-36.64	575	
40		-22.80	287	
45		- 8.99	149.1	
50	Stratopause	- 2.50	79.8	
55		-12.38	42.5	
60	Mesosphere	-26.13	22.0	
65		-39.86	10.93	Voigt
70		-53.56	5.22	
75		-64.75	2.39	
80		-74.51	1.14	
85	Mesopause	-84.26	0.45	
90	Thermosphere	-86.28	0.18	Gauss
95		-84.73	0.08	
100		-78.07	0.03	

great, and it follows that the absorption peaks are nearly independent of altitude. Actually, this is true only for fairly high pressures. As the pressure decreases to zero, the strength does continue to decrease, but the width is subject to a new phenomenon.

Formula (8) computes the "pressure-broadened" width. When it becomes very small, there are other broadening mechanisms that take over, the next of importance being Doppler broadening. This is associated with a "Gaussian" shape function and a line width equal to (with ν_o still in gigahertz)

$$\gamma_D = 1.096\ \nu_o \theta^{-1/2} \qquad \text{kHz.} \tag{9}$$

In the mesosphere it turns out that pressure-broadening and Doppler-broadening are of the same order of magnitude, and in place of either the Lorentz or Gauss functions, it is the intermediate Voigt line shape that theory will require. In Figure 1 are plotted examples of normalized Voigt profiles with both imaginary and real parts (u and v) shown. The Voigt function is hard to compute and following Olivero and Longbothum (1977) it seems an adequate

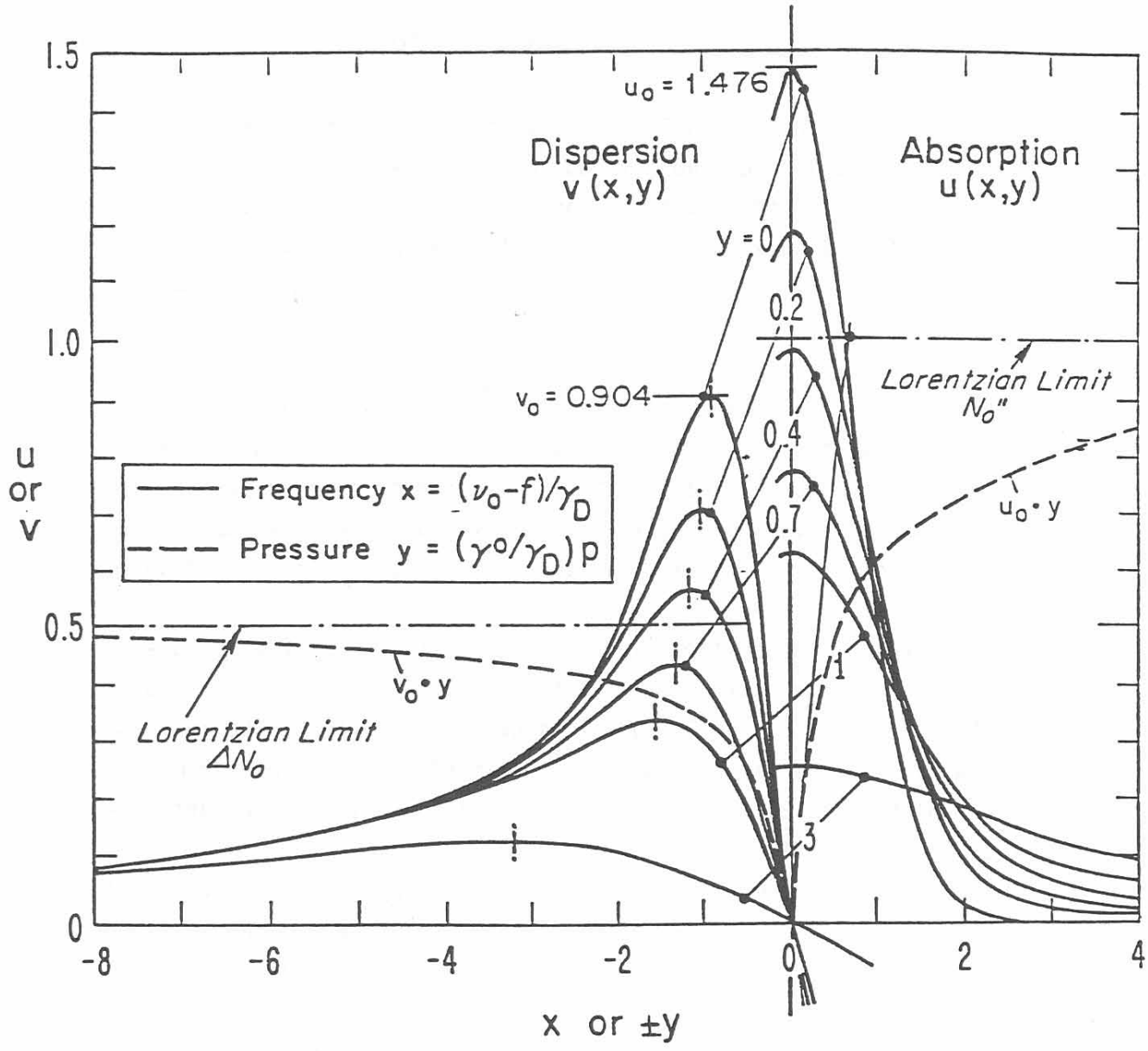

Figure 1. Normalized Voight profiles of absorption u and v. Shown are profiles versus frequency x at constant pressure y (solid curves) and the pressure profiles of maximum absorption u_o and peak dispersion v_o.

approximation to retain the Lorentz shape function and to suppose that the γ in (6) is replaced by

$$\gamma_h = 0.535\gamma + [(0.465\gamma)^2 + \gamma_D^2]^{1/2}. \qquad (10)$$

Our final model uses this last approximation with the Lorentz shape function. All told, it uses Table 1 and the formulas (5) through (10) to provide a spectrum of refractivity in the 60-GHz range under mesospheric conditions. Figure 2 shows plots of attenuation α and the dispersive part of the phase lag β for the range from 50 to 70 GHz and for conditions at about 30 km altitude.

2.2 The Geomagnetic Field and the Zeeman Effect

The Zeeman effect occurs because each of the fine structure levels is degenerate since the corresponding states have undetermined azimuthal motion. If J is the quantum number of total angular momentum, then the quantum number M of azimuthal momentum can be any integer from -J to J. Thus the degeneracy is of order 2J + 1.

When, however, the oxygen molecule is subjected to a static magnetic field, there is a force acting on the internal magnetic dipole that causes the molecule to precess about the field. This precession affects the rotational energy in a manner directly related to the azimuthal quantum number M. The level then splits into 2J + 1 new levels, and this elimination of degeneracy is called the Zeeman effect.

For transitions between those many levels there are stringent selection rules. When J changes by one, we can simultaneously have M either remaining fixed or also changing by one. Furthermore, each of those transitions can arise because of interaction with only one component of the electromagnetic field. The line components obtained when M is unchanged are called the π components and arise from interaction with a magnetic field vector that is linearly polarized in the direction of the static magnetic field. When M increases or decreases by one, the components are the σ^+ or σ^- components and are caused by interacton with a magnetic field vector that is circularly polarized in the plane perpendicular to the static magnetic field. The σ^+ components arise from a right circularly polarized field and the σ^- components from a left circularly polarized field. The convention used here is adapted

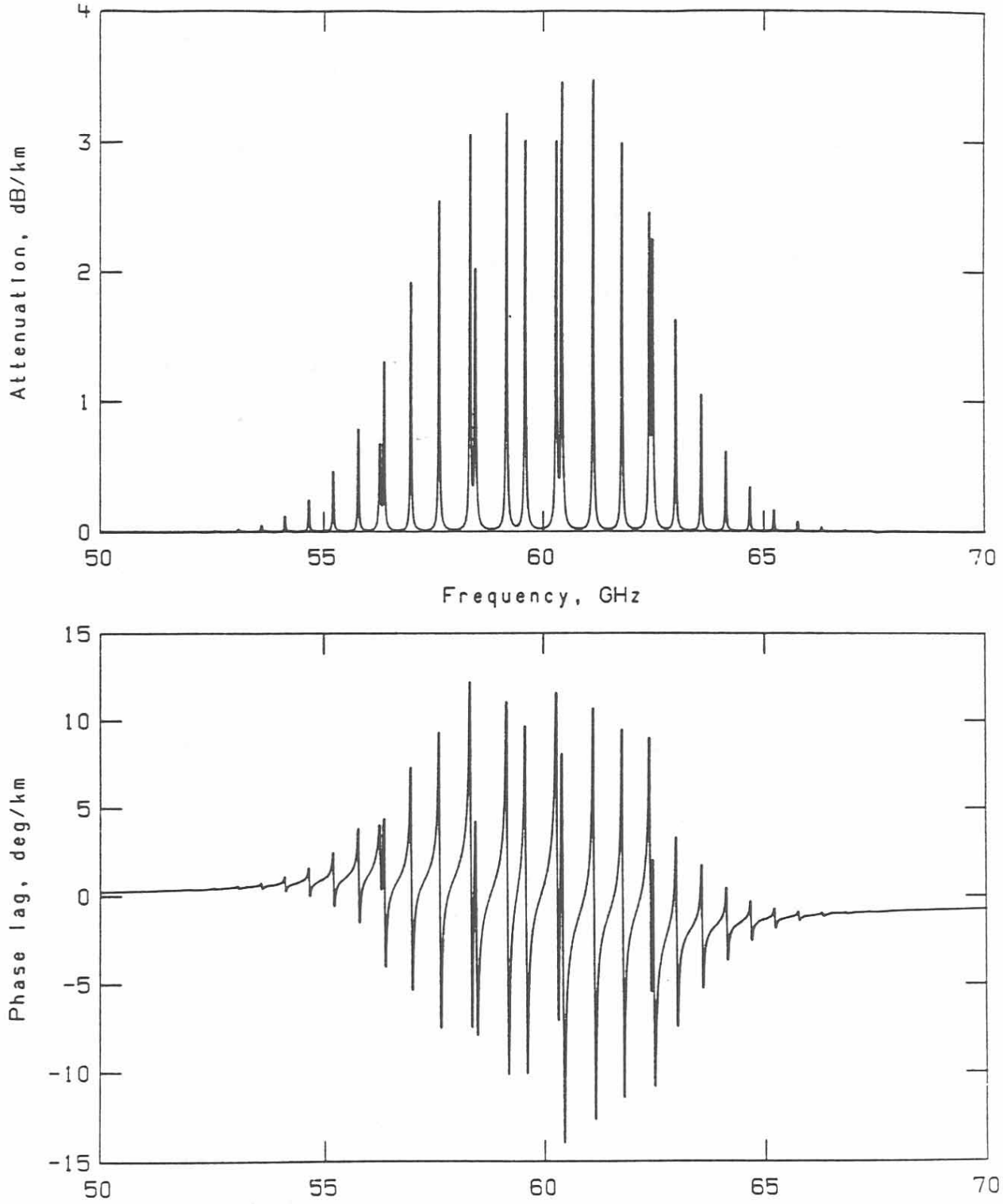

Figure 2. Pressure-broadened oxygen microwave lines in dry air for conditions at about 30 km altitude with p = w kPa, T = 225 K; at top is the attenuation spectrum and at bottom is the delay spectrum.

from the so-called IEEE convention and states that a right circularly polarized field rotates in the same direction as would a right-handed helix advancing in the direction (in this case) of the static magnetic field. That this anisotropic behavior is to be expected is suggested by noting that a force along the axis of rotation ought not to change the azimuthal motion while circularly polarized forces should do exactly that.

Figure 3 gives an example of the schematic distribution of energy levels and the allowed transitions for the case K = 3. A moment's look at this figure shows how each set of components of the K^+ line contains 2K + 1 sub-lines, while for the K^- line each set contains 2K - 1 sublines.

The line center frequency of a single Zeeman component is given by

$$\nu_o^z = \nu_o + 28.03 \cdot 10^{-6}\ \eta\ B_o \quad \text{GHz}, \tag{11}$$

where ν_o is the center frequency of the unsplit line, B_o (measured in microtesla) is the flux density of the static magnetic field, and η is a coefficient that depends on J, K, M, and ΔM. Since the geomagnetic field is on the order of 50 μT, it is large enough to spread the line by perhaps 3 MHz. In the mesosphere the magnetic field becomes an important part of the environment.

Each set of Zeeman components leads to a "refractivity" that is a function of frequency that we assume can be written as

$$N_\alpha(f) = \sum_M S\ \xi_M\ F_M(f), \tag{12}$$

where the functions F are the Lorentz shapes given in (6) and the center frequencies are in (11). The line strength S and the line width γ (or γ_h) are independent of M and equal to the values given by (7) and (10). We speak of N_o when the π components are used and of $N_\pm$ for the $\sigma^\pm$ components.

A scheme to calculate the coefficients ξ and η for the individual Zeeman components was derived from the work of Lenoir (1968) by Liebe (1981) and is described in Table 3. Numerical and graphical results for the eight lines from $1^\pm$ to $7^\pm$ are illustrated in Table 4 and Figure 4. In addition, we note that $\Sigma\xi_M$ equals 1 in the case of N_o and 1/2 for the other two. When $B_o = 0$ in (11) all the functions F_M are equal and the terms in (12) add so that

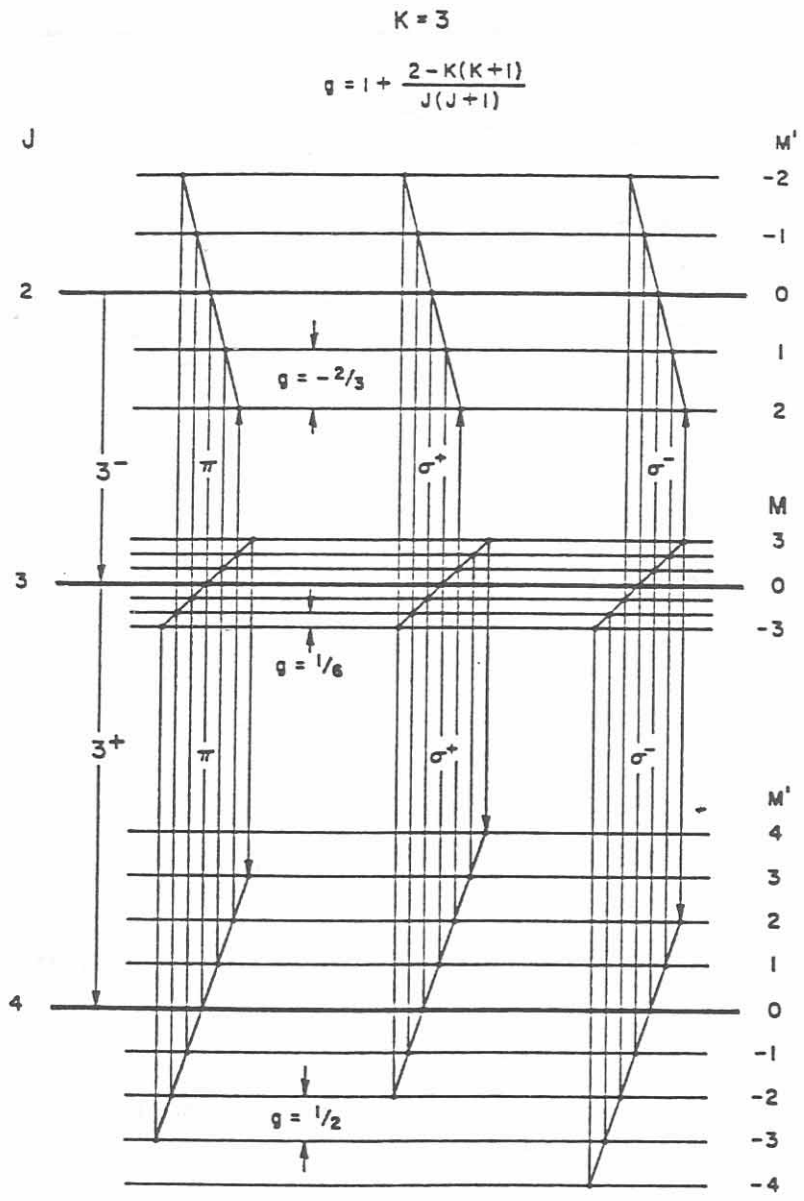

Figure 3. Schematic energy level diagram displaying the Zeeman components for the 3^+ and 3^- oxygen microwave lines. In actuality, the energy levels for J = K±1 both lie below that for J = K.

Table 3. Coefficients for the Zeeman Components.

Zeeman transitions	$\eta_M(K)$	$\xi_M(K)$	$\eta_M(K)$	$\xi_M(K)$
	$M=-K,-K+1,\ldots,K$		$M=-K+1,-K+2,\ldots,K-1$	
π $(\Delta M=0)$	$\frac{M(K-1)}{K(K+1)}$	$\frac{3((K+1)^2-M^2)}{(K+1)(2K+1)(2K+3)}$	$\frac{M(K+2)}{K(K+1)}$	$\frac{3(K^2-M^2)}{K(2K+1)(2K-1)}$
σ^+ $(\Delta M=1)$	$\frac{M(K-1)-K}{K(K+1)}$	$\frac{3(K-M+1)(K-M+2)}{4(K+1)(2K+1)(2K+3)}$	$\frac{M(K+2)-1}{K(K+1)}$	$\frac{3(K-M+1)(K-M)}{4K(2K+1)(2K-1)}$
σ^- $(\Delta M=-1)$	$\frac{M(K-1)+K}{K(K+1)}$	$\frac{3(K+M+1)(K+M+2)}{4(K+1)(2K+1)(2K+3)}$	$\frac{M(K+2)+1}{K(K+1)}$	$\frac{3(K+M+1)(K+M)}{4K(2K+1)(2K-1)}$

$$2N_+ = 2N_- = N_o = N, \tag{13}$$

where N here is just the single line as previously defined in (5) and (6).

The three patterns of specific attenuation for the lines from $1^{\pm}$ to $29^{\pm}$ have been calculated for temperatures and pressures corresponding to heights ranging from 30 to 100 km and for the two geomagnetic flux densities of 30 and 60 μT. A catalog of the complete set was presented in graphical form by Liebe (1983). A sample consisting of the 7^+ line is shown in Figure 5. We note that above 70 km the individual, now mostly Doppler-broadened, components become discernable, and that even at 40 km the three patterns are decidedly different, thus implying anisotropy.

We have referred to the three patterns as refractivities, but it is more exact to say they are components of the constitutive properties in the mesospheric atmosphere. Since it is the paramagnetic properties of oxygen that bring about the absorption lines, it is the magnetic permeability that is affected. To introduce the notation we shall use, we first note that in the usual isotropic case one expects the relative permeability to have the form

$$\mu_r = (1 + N)^2 \approx 1 + 2N,$$

where N is the refractivity and the approximation follows because N is on the order of 10^{-6}. When the medium is anisotropic, the permeability becomes a tensor of rank 2 and we would expect to write

$$\mu = \mu_o(I + 2N), \tag{14}$$

Table 4. The Frequency Shifts η and Relative Intensity Factors ξ for the Zeeman Components of the $1^{\pm}$ to $7^{\pm}$ Oxygen Lines

	K	7^+		7^-		5^+		5^-		3^+		3^-		1^+		1^-	
	M	η	ξ	η	ξ	η	ξ	η	ξ	η	ξ	η	ξ	η	ξ	η	ξ
	7	.7500	.0221														
	6	.6429	.0412	.9643	.0286												
	5	.5357	.0574	.8036	.0527	.6667	.0385										
	4	.4286	.0706	.6429	.0725	.5333	.0699	.9333	.0545								
	3	.3214	.0809	.4821	.0879	.4000	.0944	.7000	.0970	.5000	.0833						
	2	.2143	.0882	.3214	.0989	.2667	.1119	.4667	.1273	.3333	.1429	.8333	.1429				
	1	.1071	.0926	.1607	.1055	.1333	.1224	.2333	.1455	.1667	.1786	.4167	.2286	.0000	.3000		
π	0	.0000	.0941	.0000	.1077	.0000	.1259	.0000	.1515	.0000	.1905	.0000	.2571	.0000	.4000	.0000	1.0000
	-1	-.1071	.0926	-.1607	.1055	-.1333	.1224	-.2333	.1455	-.1667	.1786	-.4167	.2286	.0000	.3000		
	-2	-.2143	.0882	-.3214	.0989	-.2667	.1119	-.4667	.1273	-.3333	.1429	-.8333	.1429				
	-3	-.3214	.0809	-.4821	.0879	-.4000	.0944	-.7000	.0970	-.5000	.0833						
	-4	-.4286	.0706	-.6429	.0725	-.5333	.0699	-.9333	.0545								
	-5	-.5357	.0574	-.8036	.0527	-.6667	.0385										
	-6	-.6429	.0412	-.9643	.0286												
	-7	-.7500	.0221														
	7	.6250	.0007														
	6	.5179	.0022	.9464	.0011												
	5	.4107	.0044	.7857	.0033	.5000	.0017										
	4	.3036	.0074	.6250	.0066	.3667	.0052	.9000	.0030								
	3	.1964	.0110	.4643	.0110	.2333	.0105	.6667	.0091	.2500	.0060						
	2	.0893	.0154	.3036	.0165	.1000	.0175	.4333	.0182	.0833	.0179	.7500	.0143				
	1	-.0179	.0206	.1429	.0231	-.0333	.0262	.2000	.0303	-.0833	.0357	.3333	.0429	-.5000	.0500		
σ^+	0	-.1250	.0265	-.0179	.0308	-.1667	.0367	-.0333	.0455	-.2500	.0595	-.0833	.0857	-.5000	.1500	-.5000	.5000
	-1	-.2321	.0331	-.1786	.0396	-.3000	.0490	-.2667	.0636	-.4167	.0893	-.5000	.1429	-.5000	.3000		
	-2	-.3393	.0404	-.3393	.0495	-.4333	.0629	-.5000	.0848	-.5833	.1250	-.9167	.2143				
	-3	-.4464	.0485	-.5000	.0604	-.5667	.0787	-.7333	.1091	-.7500	.1667						
	-4	-.5536	.0574	-.6607	.0725	-.7000	.0962	-.9667	.1364								
	-5	-.6607	.0669	-.8214	.0857	-.8333	.1154										
	-6	-.7679	.0772	-.9821	.1000												
	-7	-.8750	.0882														
	7	.8750	.0882														
	6	.7679	.0772	.9821	.1000												
	5	.6607	.0669	.8214	.0857	.8333	.1154										
	4	.5536	.0574	.6607	.0725	.7000	.0962	.9667	.1364								
	3	.4464	.0485	.5000	.0604	.5667	.0787	.7333	.1091	.7500	.1667						
	2	.3393	.0404	.3393	.0495	.4333	.0629	.5000	.0848	.5833	.1250	.9167	.2143				
σ^-	1	.2321	.0331	.1786	.0396	.3000	.0490	.2667	.0636	.4167	.0893	.5000	.1429	.5000	.3000		
	0	.1250	.0265	.0179	.0308	.1667	.0367	.0333	.0455	.2500	.0595	.0833	.0857	.5000	.1500	.5000	.5000
	-1	.0179	.0206	-.1429	.0231	.0333	.0262	-.2000	.0303	.0833	.0357	-.3333	.0429	.5000	.0500		
	-2	-.0893	.0154	-.3036	.0165	-.1000	.0175	-.4333	.0182	-.0833	.0179	-.7500	.0143				
	-3	-.1964	.0110	-.4643	.0110	-.2333	.0105	-.6667	.0091	-.2500	.0060						
	-4	-.3036	.0074	-.6250	.0066	-.3667	.0052	-.9000	.0030								
	-5	-.4107	.0044	-.7857	.0033	-.5000	.0017										
	-6	-.5179	.0022	-.9464	.0011												
	-7	-.6250	.0007														

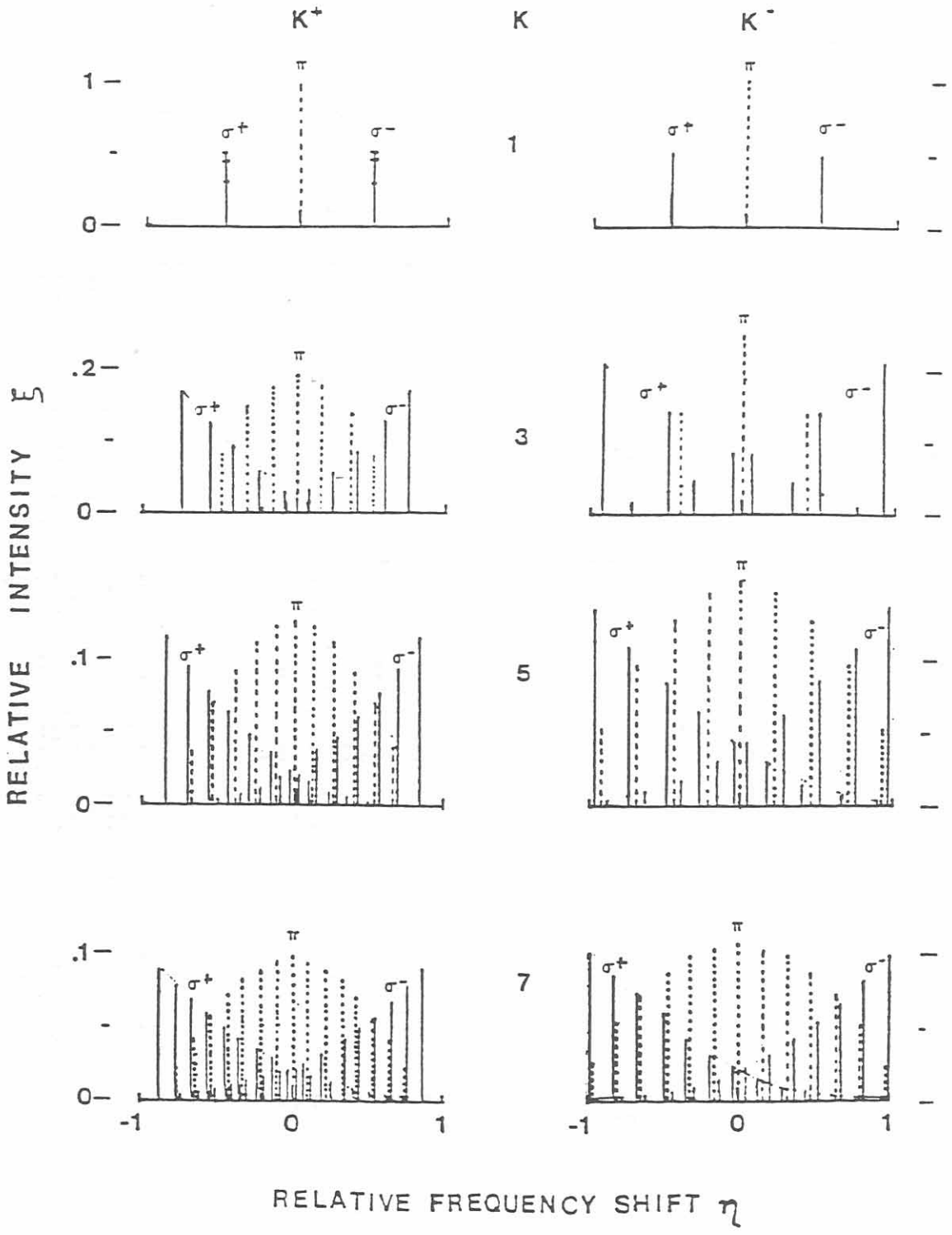

Figure 4. Schematic plots of the frequency shifts η and relative intensity factors ξ for the Zeeman components of the $1^{\pm}$ to $7^{\pm}$ oxygen lines.

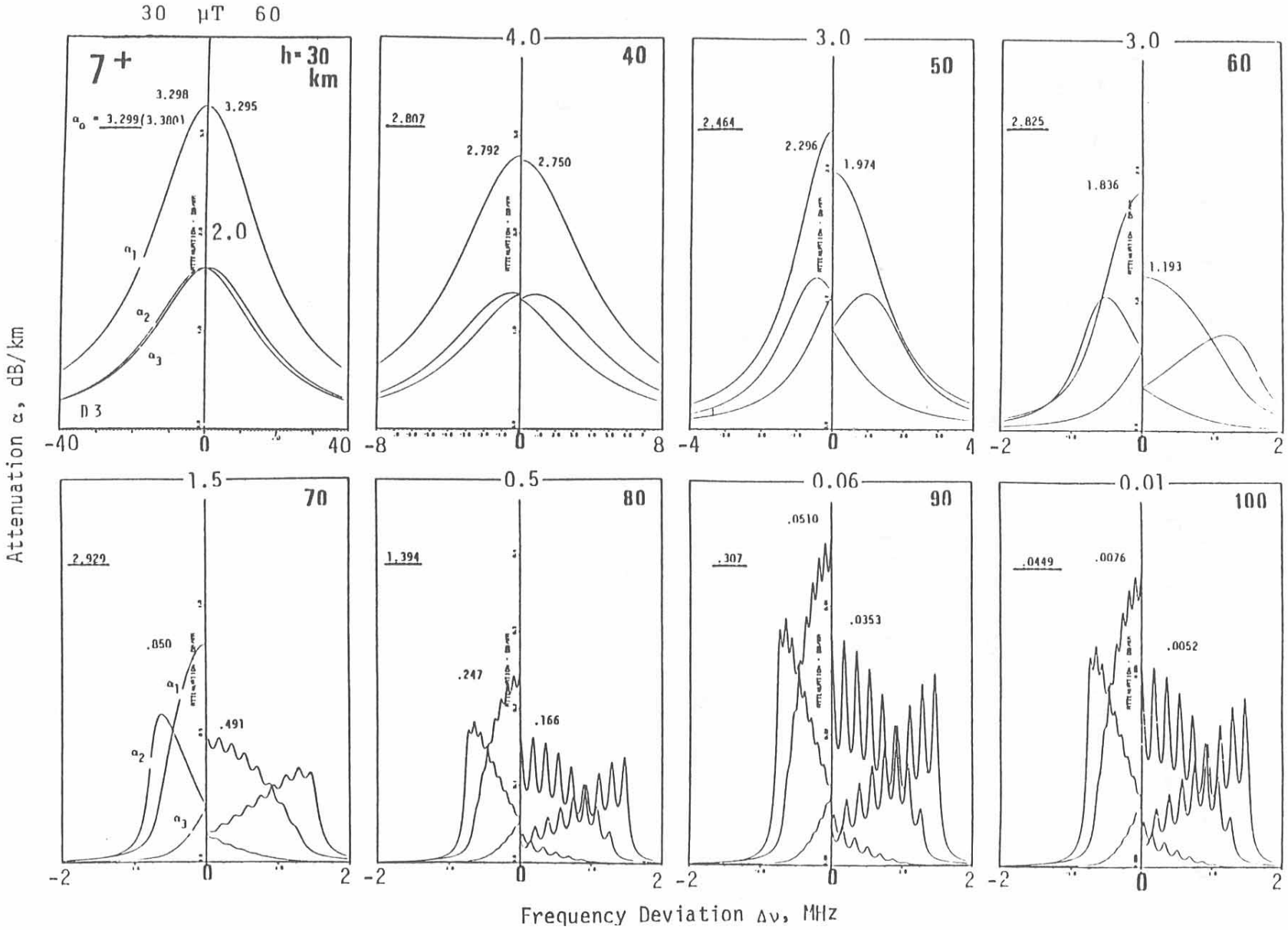

Figure 5. Attenuation patterns of the 7^+ oxygen line for altitudes from 30 to 100 km. Each frame displays the three separate patterns for magnetic flux densities of 30 and 60 μT.

where $\mu_o = 4\pi \cdot 10^{-7}$ H/m is the permeability of free space, I is the unit tensor, and **N** would be a kind of refractivity tensor.

We can represent **N** as a 3x3 matrix once we specify a coordinate system. Let $\mathbf{e}_o$ be a unit vector in the direction of the geomagnetic field, and let $\mathbf{e}_r$, $\mathbf{e}_\ell$ be vectors of unit size that represent right and left circularly polarized fields in the plane orthogonal to $\mathbf{e}_o$. Then in terms of the basis $(\mathbf{e}_r, \mathbf{e}_\ell, \mathbf{e}_o)$ the tensor **N** is represented by the diagonal matrix

$$\mathbf{N} = \begin{bmatrix} 2N_+ & 0 & 0 \\ 0 & 2N_- & 0 \\ 0 & 0 & N_o \end{bmatrix} \tag{15}$$

Turning to more customary notation, let us use the basis $(\mathbf{e}_x, \mathbf{e}_y, \mathbf{e}_o)$ where $\mathbf{e}_x$, $\mathbf{e}_y$ are real unit vectors that combine with $\mathbf{e}_o$ to form a right-handed orthogonal triad. We may write

$$\mathbf{e}_r = (\mathbf{e}_x + i\mathbf{e}_y)/\sqrt{2} \quad \text{and} \quad \mathbf{e}_\ell = (\mathbf{e}_x - i\mathbf{e}_y)/\sqrt{2}\ , \tag{16}$$

so that the transformation from the first circular components to the new linear ones is

$$\mathbf{C} = \begin{bmatrix} 1/\sqrt{2} & 1/\sqrt{2} & 0 \\ i/\sqrt{2} & -i/\sqrt{2} & 0 \\ 0 & 0 & 1 \end{bmatrix} \tag{17}$$

The refractivity tensor can now be represented by the matrix obtained through a "similarity transformation,"

$$\mathbf{N}' = \mathbf{C}\,\mathbf{N}\,\mathbf{C}^{-1} = \begin{bmatrix} N_+ + N_- & -i(N_+ - N_-) & 0 \\ i(N_+ - N_-) & N_+ + N_- & 0 \\ 0 & 0 & N_o \end{bmatrix} \tag{18}$$

where we use the conventional prime for the matrix representation in the "new coordinate system." Note that when the magnetic field B_o decreases to zero, it follows from (13) that both matrices (15) and (18) reduce to a simple refractivity times the unit matrix.